Common-Channel Optical Physical-Layer Network Coding

Ming Li, Yajun Wu, Lian-Kuan Chen, *Senior Member, IEEE*, and Soung Chang Liew, *Fellow, IEEE*

***Abstract*— We propose and experimentally demonstrate a coherent optical physical-layer network coding scheme on polarization-multiplexed differential quaternary phase-shift keying (PM-DQPSK) signals, in which the two PM-DQPSK signal components in the network-coded signal occupy the same channel and cannot be separated by conventional means of demultiplexing. In the scheme, network coding at intermediate nodes is realized by combining the two PM-DQPSK signals with a coupler. For network decoding at terminal nodes, one of the signal components is reconstructed and subtracted from the network-coded signal to obtain the other signal component. From its known bit sequence, waveform reconstruction of the signal to be subtracted is implemented by a lookup table. Carrier phase estimation for the reconstructed waveform utilizes the property that DQPSK signals have constant modulus at the sampling point. Experimental results show that, for 12-GBd PM-DQPSK signals, network decoding at a bit error rate of 10^{-3} can be achieved, with 2.1-dB optical signal-to-noise ratio penalty relative to back-to-back transmission.**

***Index Terms*— Coherent optical fiber communication, optical fiber networks, optical physical-layer network coding (PNC), quaternary phase-shift keying (QPSK).**

I. Introduction

NETWORK coding is a powerful technique to improve efficiency [1] and security [2] in communication networks. Conventionally, network coding is performed on the digital bit stream after demodulation/decoding at an intermediate node. Physical-layer network coding (PNC), on the other hand, realizes network coding directly at the physical layer as part of the demodulation and decoding process [3]. This can boost system throughput significantly [4].

Although optical PNC can be realized by all-optical logic [5], other optical PNC schemes which are more flexible have been proposed [6]–[8]. In [6], optical PNC for boosting network efficiency was demonstrated. In particular, [6] showed that full-duplex communication between optical network units (ONUs) in a time-division multiplexed passive optical network can be realized by combining the optical signals from the communicating ONUs with a coupler. In the scheme, non-return-to-zero on-off keying (NRZ-OOK) signals carried on different center wavelengths were assumed. That is, the two signal components in the network-coded signal were carried on different wavelengths. In [7], optical PNC for network protection was demonstrated. Specifically, [7] showed that optical PNC can save resources required for network protection in a multicast network. Unlike in [6], the two NRZ-OOK signal components in the network-coded signal in [7] were carried on exactly the same center wavelength. However, the two signals were combined by means of polarization multiplexing so that in the network-coded signal the two signal components were on two orthogonal polarization states. In [8], optical PNC in a star-topology fiber-wireless system to double the system throughput was demonstrated. The network coding process in [8] was similar to that in [7], except that the modulation format was changed to orthogonal frequency-division multiplexing (OFDM).

In this letter, we demonstrate common-channel optical PNC on two polarization-multiplexed differential quaternary phase-shift keying (PM-DQPSK) signals on the same wavelength. Common-channel PNC for wireless RF based on minimum-shift keying signals has been experimentally demonstrated in [9], but with significantly different decoding algorithms. In our scheme network coding is realized by simply combining the two signals with a coupler, and at the receiver the network-coded signal is coherently detected. This is "true" optical PNC because the two optical signals are on the same wavelength and they both use both the polarization states. In other words, after network coding the two signal components occupy the same channel and cannot be separated by conventional demultiplexing. Therefore, wavelength resource can be fully utilized. The key contribution of this letter is a network decoding technique that allows the recovery of the desired signal component within the overlapping signal components.

II. The Proposed Optical PNC Scheme and Experimental Setup

A. Applications of Optical Network Coding

We first quickly review a network setup in which optical network coding can be utilized – we emphasize that this is only one scenario to which optical network coding can be applied and it only serves as an illustrating example.

Consider an optical network as shown in Fig. 1(a). Nodes A and B want to broadcast signals N_1 and N_2 to both nodes C and D. In a conventional network, the signals N_1 and N_2 will need to occupy two separate channels from node E to

Manuscript received February 25, 2014; revised April 12, 2014; accepted April 30, 2014. Date of publication May 6, 2014; date of current version June 18, 2014. This work was supported in part by the Hong Kong Research Grants Council under Grant 414713, in part by the Direct Grant for Research, and in part by the University Grants Committee, Hong Kong Special Administrative Region, under Project AoE/E-02/08.

M. Li is with the Institute of Network Coding, Chinese University of Hong Kong, Hong Kong (e-mail: mingli@inc.cuhk.edu.hk).

Y. Wu, L.-K. Chen, and S. C. Liew are with the Department of Information Engineering, Chinese University of Hong Kong, Hong Kong (e-mail: wy112@ie.cuhk.edu.hk; lkchen@ie.cuhk.edu.hk; soung@ie.cuhk.edu.hk).

Color versions of one or more of the figures in this letter are available online at http://ieeexplore.ieee.org.

Digital Object Identifier 10.1109/LPT.2014.2322256

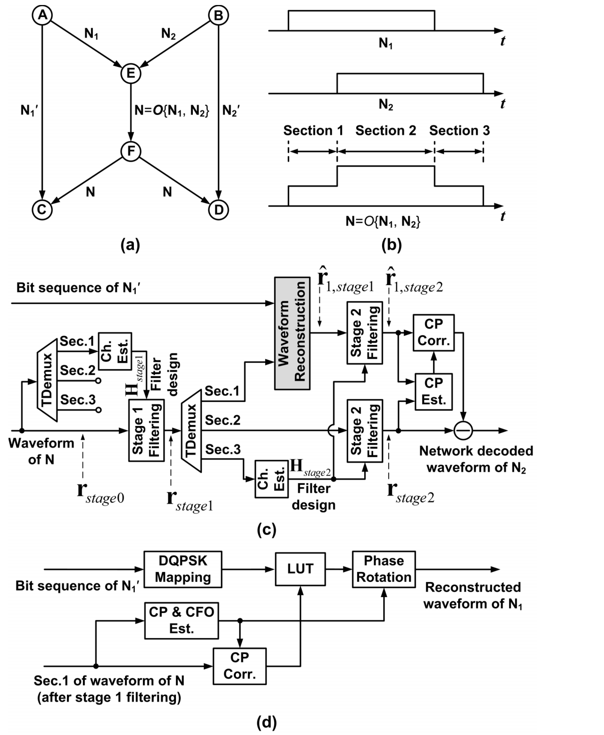

Fig. 1. (a) An illustration of a network coding scenario; (b) the packets before and after optical PNC; (c) the network decoding process; and (d) the waveform reconstruction module.

node F. With network coding, at node E signals N_1 and N_2 are combined into one signal by a network coding operation, $\mathrm{N} = O\{\mathrm{N}_1, \mathrm{N}_2\}$ and delivered over link E-F to node F. Node F then further delivers $O\{\mathrm{N}_1, \mathrm{N}_2\}$ to nodes C and D through link F-C and link F-D, respectively. Since only $\mathrm{N} = O\{\mathrm{N}_1, \mathrm{N}_2\}$ (rather than both N_1 and N_2) is transmitted across link E-F, one channel from E to F can be saved. For signal recovery at the terminal nodes, consider node C for example. Suppose that another version of N_1, denoted by $\mathrm{N}_1{}'$ in Fig. 1(a), is available at node C by another means – in Fig. 1(a), $\mathrm{N}_1{}'$ is obtained from a separate link A-C; in general, all we need is that one of the signal components is available by some means. Then, node C can recover N_2 by a network decoding process through which N_1 is removed from N using $\mathrm{N}_1{}'$. Abstractly, the network decoding process can be expressed as $\mathrm{N}_2 = D\{\mathrm{N}, \mathrm{N}_1{}'\}$.

B. Proposed Coding/Decoding Scheme for Optical PNC

The previous example illustrates the principle of network coding in general. Specifically, when network coding $O\{\cdot, \cdot\}$ at node E is realized *at the physical layer* by directly adding the waveforms of N_1 and N_2, network decoding $D\{\cdot, \cdot\}$ at node C can be performed by subtracting the reconstructed waveform of N_1 from the waveform of N. Here, by "reconstructed waveform of N_1" we mean the waveform obtained from $\mathrm{N}_1{}'$ to approximate the waveform of N_1. Ideally, it is desirable that $\mathrm{N}_1{}'$ is an exact replica of N_1. However, in practice the waveform of $\mathrm{N}_1{}'$ known to node C is the one that traverses the link A-C, and this waveform may be different from the waveform of N_1 that traverses the links A-E, E-F, and F-C. Network decoding should be performed by subtracting the latter.

Thanks to our proposed network decoding scheme (to be elaborated shortly), network coding can be realized by simply combining the two signals N_1 and N_2 with a coupler. As shown in Fig. 1(b), we intentionally make sure that the packets of N_1 and N_2 are not perfectly aligned in the time domain. In the combined network-coded signal N, the beginning part (section 1) and the end part (section 3) contain only N_1 and N_2, respectively; the lengths of section 1 and section 3 need to be long enough to ensure sufficient accuracy in channel estimations and lookup table (LUT) construction.

Consider network decoding at node C. We want to obtain N_2 by subtracting the reconstructed waveform of N_1 from the waveform of N, with the knowledge of $\mathrm{N}_1{}'$ which carries the same digital information (bits) as that carried by N_1. As shown in Fig. 1(c) and Fig. 1(d), the network decoding process can be summarized as:

Step 1: Filter the received network-coded signal $\mathbf{r}_{stage0}$ of N to get $\mathbf{r}_{stage1}$, such that within $\mathbf{r}_{stage1}$ the signal $\mathbf{r}_{1,stage1}$ associated with N_1 has minimum residual inter-symbol interference (ISI) and inter-polarization interference (IPI).

Step 2: Build an LUT based on the bit sequence of $\mathrm{N}_1{}'$ and section 1 of $\mathbf{r}_{stage1}$. Use the bit sequence of $\mathrm{N}_1{}'$ to look up the entries in the LUT, and rotate the phase of the output sequence to get the reconstructed waveform of $\hat{\mathbf{r}}_{1,stage1}$.

Step 3: Filter $\mathbf{r}_{stage1}$ to get $\mathbf{r}_{stage2}$, such that within $\mathbf{r}_{stage2}$ the signal $\mathbf{r}_{2,stage2}$ associated with N_2 has minimum residual ISI and IPI. Then filter $\hat{\mathbf{r}}_{1,stage1}$ with the same filtering characteristics to get $\hat{\mathbf{r}}_{1,stage2}$.

Step 4: Use $\mathbf{r}_{stage2}$ and $\hat{\mathbf{r}}_{1,stage2}$ to estimate the carrier phase (CP) for $\hat{\mathbf{r}}_{1,stage2}$, and subtract the CP-corrected $\hat{\mathbf{r}}_{1,stage2}$ from $\mathbf{r}_{stage2}$ to get the network-decoded waveform of N_2.

We explain the working principle of the LUT first. Each entry in the LUT contains two samples associated with (indexed by) several consecutive DQPSK symbols. Here, by "symbol" we mean the basic unit of the signal that carries information, and by "sample" we mean the value of the signal at some specific time. These samples are obtained by processing section 1 of N (shown in Fig. 1(b)). Given a sequence of DQPSK symbols $s_1\ s_2\ \cdots\ s_K$, for each s_k we can reconstruct the corresponding two samples by looking up the entry associated with $(s_{k-L}\ s_{k-L+1}\ \cdots\ s_{k+L})$, in which $2L+1$ is the total number of consecutive symbols that form the index. By concatenating all the reconstructed samples for s_k, $k = 1, \ldots, K$, the whole waveform is reconstructed. The number of entries increases exponentially with $2L+1$, which depends on the severity of ISI and IPI in N_1. Therefore, to minimize the size of the LUT, we minimize these two interferences in N_1 within N before constructing the LUT.

As shown in Fig. 1(c), in *step 1* we minimize the two interferences in N_1 within N by stage 1 filtering. The received dual-polarized network-coded signal $\mathbf{r}_{stage0}$ of N is the addition of the signals $\mathbf{r}_{1,stage0}$ and $\mathbf{r}_{2,stage0}$ of N_1 and N_2, respectively. In section 1, $\mathbf{r}_{stage0}$ contains only $\mathbf{r}_{1,stage0}$ but not $\mathbf{r}_{2,stage0}$. Therefore, we can estimate the characteristics of the desired first-stage filter—a butterfly filter in this letter—from section 1 of $\mathbf{r}_{stage0}$ to minimize the ISI and IPI in N_1. Stage 1 filtering is applied on all sections of $\mathbf{r}_{stage0}$ to obtain $\mathbf{r}_{stage1}$. Within $\mathbf{r}_{stage1}$, the signal associated with N_2 is denoted by $\mathbf{r}_{2,stage1}$. After stage 1 filtering, $\mathbf{r}_{stage1}$ is the addition of $\mathbf{r}_{1,stage1}$ and $\mathbf{r}_{2,stage1}$—i.e., the relationship between the network-coded signal and its two signal components is preserved.

As shown in Fig. 1(d), since in section 1 $\mathbf{r}_{stage1}$ contains only $\mathbf{r}_{1,stage1}$, in *step 2* we can use section 1 of $\mathbf{r}_{stage1}$ to construct the LUT entries. Because the CP of $\mathbf{r}_{1,stage1}$ is a random process, it needs to be estimated and corrected first. Then the samples of the CP-corrected $\mathbf{r}_{1,stage1}$ that correspond to the same $(s_{k-L}\ s_{k-L+1}\ \cdots\ s_{k+L})$ are averaged, the result of which is filled in the LUT entry indexed by that $(s_{k-L}\ s_{k-L+1}\ \cdots\ s_{k+L})$. After the LUT is constructed, the waveform of N_1 can be reconstructed from the bit sequence of N_1'. To account for the carrier frequency offset (CFO) of $\mathbf{r}_{1,stage1}$, we also rotate the phase of the LUT output, according to the CFO estimated from section 1 of $\mathbf{r}_{stage1}$. Finally we obtain $\hat{\mathbf{r}}_{1,stage1}$ for the reconstructed waveform of N_1.

An additional challenge is the CP estimation for the waveform of N_1 in section 2 of N, because the waveform is mixed with the waveform of N_2. We solve this problem by exploiting the property that the sampled modulus of equalized and polarization-demultiplexed N_2 is constant. Therefore, for the CP estimation of the waveform of N_1 in section 2 of N, we minimize the ISI and IPI in N_2. A subtlety is that N_1 and N_2 travel through different links, and they experience different ISI and IPI that cannot be minimized *simultaneously* in one shot.

To overcome the above problem, in *step 3* we apply a second-stage filter to both $\mathbf{r}_{stage1}$ and $\hat{\mathbf{r}}_{1,stage1}$ to get $\mathbf{r}_{stage2}$ and $\hat{\mathbf{r}}_{1,stage2}$. Similarly, the characteristics of the second-stage filter can be estimated from section 3 of $\mathbf{r}_{stage1}$, so that the ISI and IPI in the signal $\mathbf{r}_{2,stage2}$ of N_2 in $\mathbf{r}_{stage2}$ are minimized.

Then we come to *step 4*. In the ideal case $\mathbf{r}_{1,stage1} = \hat{\mathbf{r}}_{1,stage1}e^{j\varphi_1}$, where φ_1 is the CP of N_1. Because the CP is roughly constant in the time interval whose span is equal to the duration of the impulse response of the second-stage filter, $\mathbf{r}_{1,stage2} = \hat{\mathbf{r}}_{1,stage2}e^{j\varphi_1}$. Since we already have $\mathbf{r}_{stage2}$ and $\hat{\mathbf{r}}_{1,stage2}$, if φ_1 is successfully estimated we can obtain $\mathbf{r}_{2,stage2}$. With $\mathbf{r}_{stage2}$ and $\hat{\mathbf{r}}_{1,stage2}$ the CP of the waveform of N_1 in section 2 of N can be estimated as

$$\hat{\varphi}_1^{(i)} = \arg\min_{\varphi\in\Phi} \sum_{m=-M}^{M} \left\{ \left[|r_{x,stage2}^{(i+m)} - \hat{r}_{1x,stage2}^{(i+m)} e^{j\varphi}|^2 - A^2 \right]^2 + \left[|r_{y,stage2}^{(i+m)} - \hat{r}_{1y,stage2}^{(i+m)} e^{j\varphi}|^2 - A^2 \right]^2 \right\}, \quad (1)$$

where $r_{x,stage2}^{(i)}$ and $r_{y,stage2}^{(i)}$ are the i^{th} samples of the x- and y-polarized components of $\mathbf{r}_{stage2}$; $\hat{r}_{1x,stage2}^{(i)}$ and $\hat{r}_{1y,stage2}^{(i)}$ are the i^{th} samples of the x- and y-polarized components of $\hat{\mathbf{r}}_{1,stage2}$; φ is a trial CP for $\hat{\mathbf{r}}_{1,stage2}$; A is the modulus of the constellation of N_2; $2M+1$ is the number of points for moving summation; and Φ is the set of the trial phases, respectively. Since $r_{x,stage2}^{(i)} - \hat{r}_{1x,stage2}^{(i)}e^{j\varphi}$ and $r_{y,stage2}^{(i)} - \hat{r}_{1y,stage2}^{(i)}e^{j\varphi}$ are the i^{th} samples of the x- and y-polarized components of the network-decoded signal, assuming the CP of the waveform of N_1 is φ, (1) chooses the trial CP that minimizes the moving sum of the squared error between the squared modulus of the sampled network-decoded waveform of N_2 and the corresponding squared constant which is determined by the constellation of N_2.

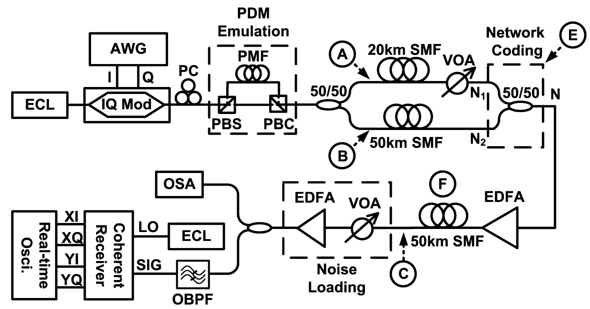

Fig. 2. Experimental setup.

C. Experimental Setup

Fig. 2 shows the experimental setup. We used an arbitrary waveform generator (AWG) to generate two independent packets, each of which consisted of 125,000-point repeated 2^{15} pseudorandom bit sequence at 12 GSa/s. Then the two independent packets were used to modulate the I and Q branches of the 1,550-nm laser emitted by a 100-kHz external cavity laser (ECL). The generated 12-GBd optical DQPSK signal was then split into two branches with a polarization beam splitter (PBS) and recombined with a polarization beam combiner (PBC) to form a PM-DQPSK signal. Between the PBS and the PBC a one-meter polarization maintaining fiber (PMF) was used to decorrelate the two branches of signals. After that, to emulate the signals of N_1 and N_2 before network coding, the PM-DQPSK signal was split into two branches and transmitted through 20-km (emulating link A-E in Fig. 1(a)) and 50-km (emulating link B-E) standard single-mode fibers (SMFs). When the powers of the two signal components in the network-coded signal are not equal, network decoding will introduce more penalty to the signal component with smaller power. In a real network implementation the powers of the two optical signals can be balanced with variable optical attenuator (VOA). In this experiment a VOA after the 20-km SMF was used, before network coding with a coupler (emulating node E). The durations of section 1 and section 3 of the network-coded signal were around 2 μs. Then the network-coded signal was amplified by an erbium-doped fiber amplifier (EDFA) and passed through another 50-km SMF to emulate the transmission in links E-F and F-C. After transmission, the network-coded signal was attenuated by a VOA and amplified by another EDFA to adjust its optical signal-to-noise ratio (OSNR). Then the network-coded signal was passed through a 0.8-nm optical bandpass filter (OBPF) to remove the out-of-band amplified spontaneous emission (ASE) noise, and detected with an integrated coherent receiver. The local oscillator (LO) was from another 100-kHz ECL. Finally the detected signal was sampled by a real-time oscilloscope and network decoding

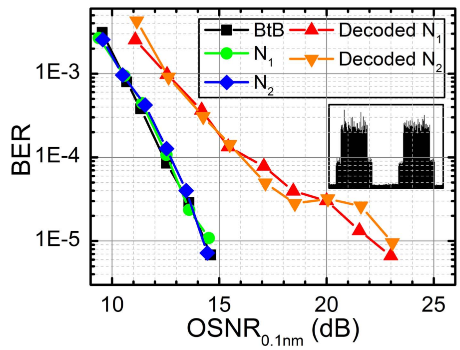

Fig. 3. BER as functions of OSNR for the cases of back-to-back (-■-), transmission in the same link, but without network coding (-●- and -◆-), and transmission with network coding and decoding (-▲- and -▼-). Inset: power waveform of the received network-coded signal.

was realized by off-line digital signal processing (DSP). For the transmission experiment for N_1' and N_2', we replaced the link between the PDM emulator and the noise loading module with a 50-km SMF. The chromatic dispersion coefficient of the SMFs is 16.5 ps/(nm·km).

In the off-line DSP, channel estimation was realized by a butterfly nine-tap feedforward equalizer (FFE) whose tap weights were updated by the constant modulus algorithm (CMA). CP estimation was realized by the Viterbi and Viterbi algorithm, and seven-point moving average was used to smooth the fourth-powered samples. CFO estimation was also based on the Viterbi and Viterbi algorithm for data modulation removal. The bit sequence of N_1' was obtained from the transmission experiment, and the LUT for waveform reconstruction considered 64 different combinations of three consecutive symbols. With 2-μs section 1 of the network-coded signal, roughly 290 samples were averaged for each of the two samples in each LUT entry. For the CP estimation of the waveform of N_1 in section 2 of the waveform of N, the set Φ of trial phases consisted of 64 phases equally distributed between $-\pi$ and π, and 25-point moving sum was used to smooth the squared error. Bit error rate (BER) was determined by counting errors out of roughly two million transmitted bits.

III. Results and Discussions

The inset of Fig. 3 shows the power waveform of the received network-coded signal. From it the three sections of the network-coded signal could be determined. Then the signal was network decoded with the proposed algorithm. Fig. 3 shows the BER as functions of OSNR in different cases. When only the 20-km branch has signal (N_1), or the 50-km branch has signal (N_2), the BER curves nearly coincide with that for the case of back to back (BtB), in which points A and C in Fig. 2 are connected directly. The required OSNR for a BER of 10^{-3} is roughly 10.5 dB. With the proposed algorithm, N_2 was successfully network decoded from section 2 of the waveform of N and the bit sequence of N_1'. At 10^{-3} BER, the required OSNR, defined as the ratio between *the power of* N_2 and the power of the optical ASE noise within 0.1-nm bandwidth, is less than 12.6 dB. Network decoding for N_1 was realized by the same DSP program with the received samples reversed in time domain. The performance of network decoding for N_1 is similar to that for N_2, and a BER of 10^{-3} can also be achieved with 12.6-dB OSNR. For both the decoding of N_1 and N_2 the OSNR penalty at 10^{-3} BER is 2.1 dB. Based on further experimental results (not shown in Fig. 3), when the power difference between N_1 and N_2 is 1.5 dB, the required OSNR for the signal component with lower power to achieve 10^{-3} BER is 14.8 dB, which is 2.2 dB higher than that for the case when the powers of the two signal components are balanced.

IV. Conclusion

We have proposed a common-channel optical PNC scheme for PM-DQPSK signals. In the scheme, network coding is realized with a coupler that combines two PM-DQPSK signals. Symbol-level time-domain synchronization is not required. Although the two signal components in the network-coded signal occupy the same channel and cannot be separated by conventional means of demultiplexing, utilizing the knowledge of the bit sequence of one signal component, the other signal component is successfully obtained by network decoding. For 12-GBd PM-DQPSK signal, we have experimentally demonstrated network coding and decoding with 2.1-dB OSNR penalty at 10^{-3} BER, relative to back-to-back transmission.

Acknowledgment

The authors would like to thank NeoPhotonics for providing the coherent receiver for this study.

References

[1] S.-Y. R. Li, R. W. Yeung, and N. Cai, “Linear network coding,” *IEEE Trans. Inf. Theory*, vol. 49, no. 2, pp. 371–381, Feb. 2003.
[2] N. Cai and R. W. Yeung, “Secure network coding,” in *Proc. IEEE ISIT*, Lausanne, Switzerland, Jun. 2002, pp. 323.
[3] S. Zhang, S. C. Liew, and P. P. Lam, “Hot topic: Physical-layer network coding,” in *Proc. 12th Annu. ACM Int. Conf. Mobile Comput. Netw.*, Los Angeles, CA, USA, Sep. 2006, pp. 358–365.
[4] S. C. Liew, S. Zhang, and L. Lu, “Physical-layer network coding: Tutorial, survey, and beyond,” *Phys. Commun.*, vol. 6, pp. 4–42, Mar. 2013.
[5] Y. An, F. D. Ros, and C. Peucheret, “All-optical network coding for DPSK signals,” in *Proc. OFC*, Anaheim, CA, USA, Mar. 2013, paper JW2A.60.
[6] Q. Wang, K.-H. Tse, L.-K. Chen, and S. C. Liew, “Physical-layer network coding for VPN in TDM-PON,” *IEEE Photon. Technol. Lett.*, vol. 24, no. 23, pp. 2166–2168, Dec. 1, 2012.
[7] Z. X. Liu, M. Li, L. Lu, C.-K. Chan, S. C. Liew, and L.-K. Chen, “Optical physical-layer network coding,” *IEEE Photon. Technol. Lett.*, vol. 24, no. 16, pp. 1424–1427, Aug. 15, 2012.
[8] Z. X. Liu, L. Lu, L. Z. You, C.-K. Chan, and S. C. Liew, “Optical physical-layer network coding over fiber-wireless,” in *Proc. 39th ECOC*, London, U.K., Sep. 2013, pp. 1–4, paper Mo.3.F.3.
[9] S. Katti, S. Gollakota, and D. Katabi, “Embracing wireless interference: Analog network coding,” in *Proc. ACM SIGCOMM*, Kyoto, Japan, Aug. 2007, pp. 397–408.